Author Manuscript

Author Manuscript

Author Manuscript

Author Manuscript

HHS Public Access

Author manuscript

J Orthop Res. Author manuscript; available in PMC 2019 December 01.

Published in final edited form as:

J Orthop Res. 2018 December ; 36(12): 3275–3284. doi:10.1002/jor.24122.

Genetic Lineage Tracing of Targeted Cell Populations During Enthesis Healing

Helen L. Moser[1,2], **Anton Ph. Doe**[1], **Kristen Meier**[1], **Simon Garnier**[3], **Damien Laudier**[1], **Haruhiko Akiyama**[4], **Matthias A. Zumstein**[2], **Leesa M. Galatz**[1], and **Alice H. Huang**[1]

[1]Department of Orthopaedics, Icahn School of Medicine at Mount Sinai, New York, NY 10029, USA [2]Shoulder, Elbow and Orthopaedic Sports Medicine, Department of Orthopaedic Surgery and Traumatology, Inselspital, Bern University Hospital, University of Bern, 3010 Bern, Switzerland [3]Department of Biological Sciences, New Jersey Institute of Technology, Newark, NJ 07102, USA [4]Department of Orthopaedic Surgery, Gifu University School of Medicine Gifu, Gifu Prefecture, Japan

Abstract

Rotator cuff supraspinatus tendon injuries are clinically challenging due to the high rates of failure after surgical repair. One key limitation to functional healing is the failure to regenerate the enthesis transition between tendon and bone, which heals by disorganized scar formation. Using two models of supraspinatus tendon injury in mouse (partial tear and full detachment/repair), the purpose of the study was to determine functional gait outcomes and identify the origin of the cells that mediate healing. Consistent with previous reports, enthesis injuries did not regenerate; partial tear resulted in a localized scar defect adjacent to intact enthesis, while full detachment with repair resulted in full disruption of enthesis alignment and massive scar formation between tendon and enthesis fibrocartilage. Although gait after partial tear injury was largely normal, gait was permanently impaired after full detachment/repair. Genetic lineage tracing of intrinsic tendon and cartilage/fibrocartilage cells ($Scx^{CreERT2}$ and $Sox9^{CreERT2}$, respectively), myofibroblasts ($\alpha SMA^{CreERT2}$), and Wnt-responsive stem cells ($Axin2^{CreERT2}$) failed to identify scar-forming cells in partial tear injury. Unmineralized enthesis fibrocartilage was strongly labeled by $Sox9^{CreERT2}$ while $Axin2^{CrERT2}$ labeled a subset of tendon cells away from the skeletal insertion site. In contrast to the partial tear model, $Axin2^{CreERT2}$ labeling showed considerable contribution of $Axin2^{lin}$ cells to the scar after full detachment/repair. **Clinical significance:** Clinically relevant models of rotator cuff tendon injuries in mouse enable the use of genetic tools; lineage tracing

Corresponding Author: Alice Huang, Ph.D., Assistant Professor, Icahn School of Medicine at Mount Sinai, Department of Orthopaedics, 1 Gustave Levy Place, Box 1188, New York, NY 10029, Phone: (212) 241-1158, Fax: (212) 876-3168, Alice.Huang@mssm.edu.

Authors Contribution:

HM, LG, AD, DL, and KS contributed to animal surgery, experimental assays, and data collection. Data analysis was carried out by HM and AD. Statistical analysis was carried out by SG and HM. HM, AH, LG, and MZ contributed to conception, experimental design, and data interpretation. HA created and provided the Sox9CreERT2 mouse. HM, AH, LG, and MZ prepared and edited the manuscript prior to submission.

DISCLOSURES

HM (none), AD (none), KS (none), SG (none), DL (none), MZ (Medacta International, Angiocrine Biosciences), LG (none), AHH (none).

Author Manuscript Author Manuscript Author Manuscript Author Manuscript

suggests that distinct mechanisms of healing are activated with full detachment/repair injuries vs partial tear.

Keywords

Rotator Cuff; Tendon; Enthesis; Injury; Healing

INTRODUCTION

The rotator cuff is composed of four muscles and tendons that function in concert to stabilize the glenohumeral joint. Rotator cuff tendon injuries are a common clinical problem, resulting in over 4.5 million physician visits annually.[1] These injuries often arise with aging as well as chronic overuse, which can lead to degeneration and finally rupture of one or more tendons.[2, 3] After rupture, shoulder function is impaired, indicated by weakness, decreased range of motion, and pain. Of the four tendons, the supraspinatus tendon is the most frequently injured. This is likely due to its unique location beneath the acromion bone. The supraspinatus functions to elevate the arm, and during this motion, the tendon may impinge against the acromion which predisposes this tendon for injury over time. While surgical repair of torn tendon to its bony site of attachment remains the gold standard of treatment, outcome measures can be variable and failure rates high in certain populations, despite advancements in operation technology.[4–11]

One of the key limitations in rotator cuff tendon healing is the failure to regenerate a truly functional attachment between tendon and bone. In healthy tissues, the tendon is connected to bone via a gradient of tendon, unmineralized fibrocartilage, mineralized fibrocartilage, and bone. This specialized gradient (the enthesis), functions to dissipate the high stresses that arise from the attachment of two mechanically dissimilar materials (tendon and bone).[12] While surgical repair brings the tendon back in close proximity to bone, the enthesis is never re-formed, but is replaced by disorganized scar with inferior structural and mechanical properties.[13] A number of approaches have been used to improve enthesis healing, including implantation of engineered tissue, biomaterials, or growth factors/small molecules;[14] however, none of these strategies have been effective in fully restoring enthesis structure or function. Developing new therapies that mitigate scar formation while promoting regeneration will likely require an improved understanding of the biological mechanisms that underlie enthesis healing.

Toward that end, animal models are frequently used to study supraspinatus tendon degeneration, injury, and repair. Of these models, the rodent rotator cuff has emerged as the leading model due to anatomical similarity to human. Like humans, the supraspinatus tendons of rodents are intraarticular and lie underneath the acromion. The collagen architecture of the insertion is also interdigitated.[15] While there have been numerous excellent studies of rotator cuff degeneration/injuries in rats,[16–20] genetic perturbations are difficult to achieve in rats due to the paucity of available molecular tools. Recently, a few groups established models of clinically relevant supraspinatus tendon injuries in the mouse,

Author Manuscript Author Manuscript Author Manuscript Author Manuscript

[21–24] thus opening the door for mechanistic studies enabled by the wide array of genetic tools available for mouse.

Using lineage tracing tools, a few groups are beginning to define useful markers for identifying distinct cell populations within the rotator cuff and follow their fate after tendon or enthesis injury.[22, 25–27] In our study, we used four inducible Cre lines that have not been previously evaluated for rotator cuff and determined functional outcomes and cellular mediators of healing in two injury models (partial tendon tear and full tendon detachment with surgical repair). Cre lines were selected to target tendon ($Scx^{CreERT2}$), cartilage/fibrocartilage ($Sox9^{CreERT2}$), myofibroblast ($\alpha SMA^{CreERT2}$), and putative stem cells ($Axin2^{CreERT2}$). Although multipotent, self-renewing cells have been isolated from tendon, the source and identity of these cells, their location, and *in vivo* activity remain poorly defined due to the absence of definitive markers.[28–31] It is also unclear whether the enthesis may have a source of resident stem cells that mediate healing. Since stem cells for many tissues (such as mammary gland,[32] intestinal crypt,[33] hair follicle,[34] and nail[35]) require Wnt signaling, the inducible Cre for *Axin2* (a reporter of Wnt signaling) has been successfully used to identify Wnt-responsive stem cells in many of these tissues.[32]

MATERIALS AND METHODS

Mice

All procedures were carried out according to IACUC guidelines. Mice were housed in virus free animal facilities and veterinary care provided by the Center of Comparative Medicine and Surgery at Mount Sinai. For lineage tracing, existing mouse lines were used, including $Scx^{CreERT2}$ (generated by Dr. Ronen Schweitzer), $Sox9^{CreERT2}$[36], $\alpha SMA^{CreERT2}$[37], $Axin2^{CreERT2}$[32], and the *Ai14 Rosa26-TdTomato* Cre reporter (*RosaT*).[38] Lineage tracing using these inducible Cre lines was carried out by three consecutive daily tamoxifen injections given by intraperitoneal injection (100mg/kg, Sigma) one week prior to injury.

Experimental Design

For lineage tracing, *CreERT2/RosaT* mice were used for a total of n=36 mice (n=9 per *CreERT2* line). Shoulders were harvested post-injury at d7 (n=2), d14 (n=3) and d28 (n=4) for histological analysis and cell quantification (d14 and d28 only). EdU was injected (0.05 mg, Life Technologies) at 28h, 20h, and 4h prior to harvest to label proliferating cells. Three injections of EdU were given to capture all proliferating cells within the timeframe since cell proliferation is low in adult stages. Additional wild type mice (n=32) were used for gait, radiographs, and DEXA imaging. For the repair group, $Sox9^{CreERT2}$ and $Axin2^{CreERT2}$ animals (n=5) were used for lineage tracing at d28 and gait analysis (Fig 1A, Table S1).

Supraspinatus Tendon Partial Tear Model

Even numbers of male and female mice (total n=68) were used for partial tear surgeries (average age 14.8±3.6 weeks). At time of surgery, mice were anaesthetized with 4% isofluorane, which was maintained at 2% throughout surgery. To access the supraspinatus, mice were positioned with the left forelimb in external rotation; the shoulder was then shaved and disinfected with povidone iodine and alcohol. The deltoid muscle was visualized

Author Manuscript Author Manuscript Author Manuscript Author Manuscript

by incision through the skin and detached from the acromion to expose the supraspinatus tendon. Partial tear injury was carried out by inserting a 26G syringe needle through the central portion of the supraspinatus tendon into the insertion site (Fig 1B).[22] The deltoid was then sutured back to the acromion and the skin closed. On the contralateral control side, a sham procedure was carried out (detachment and reattachment of the deltoid muscle only). Post-operative pain was managed with Buprenorphine (0.5mg/kg), consistent with IACUC guidelines.

Supraspinatus Tendon Full Detachment and Repair Model

Even numbers of male and female mice (n=10) were used for full detachment and repair surgeries (average age 19.9± 4.5 weeks). Animals were prepped for surgery as described above. After detachment of the deltoid muscle from the acromion, a 6–0 suture (Henry Schein) was placed around the acromion to retract and expose the supraspinatus and infraspinatus muscles and tendons. To hold the suprapinatus tendon prior to detachment, a suture was looped and inserted through the tendon near the myotendinous junction. The supraspinatus tendon was then detached using a No. 10 blade. For reattachment repair, a tunnel through the humeral head was made using a 26G needle. The suture holding the supraspinatus tendon was then threaded through the tunnel and the ends knotted to position the supraspinatus tendon back against the insertion. Finally, the deltoid muscle was sutured back to the acromion and the skin closed. All animals showed normal cage behavior the day after surgery.

Gait Analysis

Gait was carried out at d3, d7, d14, and d28 after injury (DigiGait Imaging System, Mouse Species Inc.). Without pretraining, mice were gaited at 10 cm/s for 4 s. Forelimb measurements were used to calculate %BrakeStance, %PropelStance, and PawArea. These parameters were chosen based on previous work in the literature as well as preliminary studies.[21, 39] Uninjured mice were also gaited to determine non-injured control values.

Histology and Immunofluorescence Analysis

Forelimbs were fixed in 4% paraformaldehyde, decalcified in EDTA, infiltrated with 5% and 30% sucrose, and frozen in OCT. Alternating coronal cryosections (12 μm) through the shoulder were collected. Immunostaining of tissues harvested at d28 was carried out using antibodies against Laminin (L9393, Sigma), α-smooth muscle actin (αSMA, C6198, Sigma) and Sca1 (AF1226, R&D Systems) with Cy3 secondary detection (711-166-152, Jackson Immuno Research) and DAPI counterstaining. EdU detection of proliferating cells was performed according to manufacturer's directions (Life Technologies). For morphological analysis and orientation of immunofluorescence images, Toluidine Blue staining was performed on adjacent sections. For plastic sectioning, samples were fixed in zinc formalin, dehydrated and infiltrated with methacrylate monomer and embedded. Plastic sections were acquired at 6μm and stained with Toludine Blue. All images were acquired using the Zeiss AxioImager microscope, with Apotome for optical sectioning of fluorescent images. Image processing was carried out using Adobe Photoshop CS6.

Author Manuscript Author Manuscript Author Manuscript Author Manuscript

Cell Quantification

The region of interest encompassing injured and uninjured enthesis was defined as shown in Fig 1C, D, and the total number of DAPI+ nuclei counted (Zeiss ZEN software). *TdTomato*+ cells were quantified in the same section to determine *CreERT2* labeled cells and reported as a percentage of total cells (*TdTomato*/DAPI).

Bone Mineral Density Analysis

Bone mineral density analysis was carried out using the Faxitron PathVision Machine measuring DEXA. After a whole shoulder radiograph was captured, all soft tissue was removed and the humeri placed into the Faxitron for further analysis. We standardized the region of interest to include the humeral head and greater tuberosity. The area of interest was reported relative to the entire humerus for bone mineral density (Fig S1).

Statistical Analysis

For gait analysis, we compared injury vs sham control and repair vs uninjured control using a linear mixed-effects model with side (injury or control) and timepoint (d3, 7, 14 and 28) as independent variables, with gait parameters as dependent variables. Mouse ID was set as a random variable to control for repeated measurements. In addition, average paw area was compared for each timepoint to limbs from uninjured control animals, using Wilcoxon rank sum tests with continuity correction. The variance of the paw area was also compared using the Bartlett test of homogeneity of variances.

For cell quantification, injury vs sham control was tested using a linear mixed-effects model with side (injury or sham) and timepoint (14 and 28) as independent variables, and log-transformed cell density or square-root-transformed %TdTomato as the dependent variables. Mouse ID was set as a random variable to control for repeated measurements.

For all linear mixed-effects models, a comparison using the Akaike Information Criterion of models with and without an interaction term between side and timepoint showed that the model without interaction was the most appropriate to describe the data. In addition, residuals for all models were inspected graphically for normality.

Statistical analyses were performed using R software (version 3.4.4).[40] Linear mixed-effects models were calculated using the lme4 package.[41]

RESULTS

Functional gait is minimally affected by partial supraspinatus tear injury

To determine the functional consequences of partial supraspinatus tendon injury, we gaited mice from d3 to d28 after injury and compared injured forelimb parameters relative to sham control and non-injured animals. While our previous gait results for the hindlimb Achilles tendon showed that parameters related to brake and propel phases of gait were most correlated with injury and healing,[39] analysis of the forelimbs did not reveal any change in brake or propel as a function of time or relative to non-injured or sham limbs (Fig 2A–D). While paw area of both limbs increased with time from d3 to d28 ($p=0.013$), there were no

Author Manuscript Author Manuscript Author Manuscript Author Manuscript

differences detected between the injured and sham limbs at any timepoint, or relative to non-injured d0 control limbs (Fig 2E, F). Using the Bartlett test, we observed increased variance in the paw area of injured limbs relative to non-injured limbs. Interestingly, variance in the sham limb relative to the non-injured limb also increased at timepoints d7 and onward. These results suggest that gait is relatively unaffected by partial tear injury.

The partially injured enthesis heals by a disorganized, hypercellular scar

Since gait appeared mostly normal, we examined the injured region of the enthesis to determine the extent of healing and the structural consequences of partial tear injury. Sections through the injured enthesis were analyzed using toluidine blue staining, which highlighted the fibrocartilaginous enthesis zone in purple. While sham controls showed normal architecture with rounded columnar cells and intense toluidine blue staining, the injured enthesis showed a region of hypercellular tissue that was not stained by toluidine blue (Fig 3A, B). This region was directly adjacent to intact enthesis, suggesting that partial tear injury resulted in scar formation and loss of normal architecture. To quantify cellularity, a region of interest was selected as described in the methods (Fig 1D) and DAPI-stained nuclei quantified at d14 and d28. At both timepoints, we observed increased cell density ($p<0.001$) relative to sham enthesis (Fig 3C). EdU staining for proliferating cells showed very few proliferating cells in the enthesis at d7; EdU+ cells at this stage were only localized to the scar area (Fig 3D, E). By d14 and d28, there was no longer any cell proliferation in the enthesis, although extensive proliferation was found in bone marrow and in the bursal/muscle tissues (Fig 3F–I). We did not observe proliferating cells in the tendon body at any timepoint. These data suggest that despite normal gait, partial tear injury induced rapid healing by disorganized, hypercellular scar formation.

Genetic lineage tracing did not identify scar forming cells

To determine whether scar-forming cells originate from adjacent tissues that de-differentiate, we used the inducible $Scx^{CreERT2}$ and $Sox9^{CreERT2}$ lines to target tendon and cartilage/fibrocartilage cells, respectively (Fig 4A–F). Control limbs labeled by $Scx^{CreERT2}$ showed robust *TdTomato* expression in the tendon body with limited labeling of enthesis cells. In contrast, labeling with $Sox9^{CreERT2}$ showed strong *TdTomato* expression in the articular cartilage of the humeral head, most of the unmineralized enthesis fibrocartilage, and tendon cells near the insertion (Fig 4C, E, S2). Sections through injured $Scx^{CreERT2}$ and $Sox9^{CreERT2}$ limbs showed that the hypercellular scar region was largely devoid of *TdTomato*+ cells (although a few were observed, yellow arrows). Overall this data suggests that scar-forming cells are not predominantly derived from tendon, articular cartilage, or unmineralized enthesis; however, the scar population may be composed of multiple lineages (Fig 4D, F, S2).

Since previous studies showed that αSMA+ cells are activated and recruited after rotator cuff, patellar, and Achilles tendon injuries,[22, 39] we used the $\alpha SMA^{CreERT2}$ to determine whether these cells contribute to the enthesis scar. Surprisingly, $\alpha SMA^{CreERT2}$ did not label epitenon cells surrounding the supraspinatus tendon (in contrast to previous studies in patellar tendon).[42] Sporadic labeling in d28 sham controls was largely restricted to the fibrotic cells of the injured deltoid muscle and periosteal cells surrounding the acromion

Author Manuscript Author Manuscript Author Manuscript Author Manuscript

bone (Fig 4G). In d28 tendon injury samples, the scar regions were completely devoid of *TdTomato*+ cells, indicating that scar cells also do not originate from αSMA^{lin} (Fig 4H). These results were further supported by immunostaining with an antibody against αSMA, which showed distinctive staining of blood vessels, but no staining in epitenon or enthesis scar cells (Fig S3).

Finally, we used $Axin2^{CreERT2}$ to identify potential resident stem cells. While $Axin2^{CreERT2}$ labeled a sub-population of tendon cells within the tendon body, very few enthesis cells were labeled and scar cells were not labeled (Fig 4I, J). This data suggests that resident enthesis stem cell populations either do not require Wnt signaling or there is no such population for the enthesis.

Quantification of *TdTomato* cells from these four inducible Cre lines showed the relative contribution of different cell lineages to the enthesis. Consistent with qualitative observations, $Sox9^{CreERT2}$ showed most efficient labeling while $\alpha SMA^{CreERT2}$ labeled cells were nearly undetectable within this region. Statistical analyses did not reveal significant differences between the control and injured regions of interest at any timepoint for $Sox9^{CreERT2}$ ($p=0.095$), $Axin2^{CreERT2}$ ($p>0.1$), or $\alpha SMA^{CreERT2}$ ($p=0.072$). Cell counting of Scx^{lin} cells however, did show that the amount of Scx^{lin} cells is significantly lower on the surgical side rleative to the sham control, independent of timepoint ($p=0.032$, Fig 4K).

Laminin and Sca1 immunostaining detected in epitenon but not scar cells

Since lineage tracing failed to identify the origin of scar cells, we carried out additional immunostaining for laminin (epitenon marker) and Sca1 (mesenchymal stem cell marker). Strong staining for laminin was detected in the muscle connective tissues (not shown), bone marrow, epitenon, and adjacent bursa with no staining detected in tendon cells, enthesis cells, or scar cells (Fig 5A, B). While Sca1 staining was also observed in epitenon, bursa, and bone marrow, there was unexpected staining in tendon cells away from the skeletal insertion (Fig 5C, D). Tendon cells near the insertion, enthesis cells and scar cells were completely negative for Sca1.

Bone mineral density is not affected by partial tear injury

To determine whether partial tear leads to alterations in bone, DEXA was performed on the whole shoulder at d56 (Fig S4). Quantification of bone mineral density in the humeral head did not reveal any differences between sham and injury, and no differences were observed with respect to sex ($p>0.1$). Radiographs also did not show ectopic ossification within or near the injured tendon (not shown).

Functional gait is permanently impaired after full tendon detachment and repair

Although the partial tendon tear model allowed us to easily identify a localized injury site, full detachment with surgical repair better models clinical practice. We therefore determined functional gait properties in this model and found that repaired forelimbs and contralateral controls were both impaired after injury relative to uninjured animals (Fig 6A). Paw area was significantly greater for both limbs compared to uninjured animals (d0) at all timepoints

Author Manuscript Author Manuscript Author Manuscript Author Manuscript

except d7 ($p<0.05$), with no differences between control and repaired limbs ($p>0.1$) at any timepoint.

At d28, gross analysis of repaired shoulders showed that the surgical repair remained intact for all mice. Toluidine blue staining showed healing of the repaired supraspinatus tendon, but not to its original insertion site (Fig 6B, C). We observed massive scar tissue around the enthesis between the tendon stump and the bone. While the original enthesis could be identified by toluidine blue staining, this residual enthesis displayed a loss of its characteristic architecture and orientation. In contrast to the partial tear, the hypercellular scar was not observed within the enthesis itself. To determine whether the scar in the repair was similar to the partial tear scar, we carried out lineage tracing with $Sox9^{CreERT2}$ and $Axin2^{CreERT2}$. Similar to previous results, $Sox9^{CreERT2}$ labeled much of the unmineralized enthesis fibrocartilage while $Axin2^{CreERT2}$ showed little labeling. However, while $Sox9^{lin}$ cells were only sporadically observed in the scar (which may again suggest that the scar is composed of multiple lineages), the majority of scar cells were $Axin2^{lin}$ (Fig 6D, E). This data indicates distinctive mechanisms of healing between the partial tear and full detachment/repair models.

DISCUSSION

In this study, we used two models of supraspinatus tendon injury and determined functional outcomes and cellular responses during healing. Our results showed that full tendon detachment with repair resulted in permanent disruption of gait in injured mice relative to non-injured mice, while gait was largely normal after partial tear. Although the tendon was re-attached after full detachment, the surgical process required for the repair (such as drilling into the humeral head) likely caused an additional injury response and influx of new cells from the bone marrow. Although inflammatory markers and local immune cells were not determined, the additional injury may exacerbate local inflammation, resulting in poorer functional outcomes. Indeed, histological sections through the defect showed massive scar formation and loss of characteristic enthesis organization and orientation in this model, even though repairs remained intact. In contrast, the less severe injury in the partial tear model allowed for easy identification of a very localized defect site within the enthesis, which was hypercellular and disorganized compared to native adjacent enthesis (which appeared normal). The choice of injury models will depend on the specific scientific question; although the repair injury better models clinical practice and results in significant loss of function (which may be a useful feature for testing therapeutics), the partial tear model requires less technical expertise. The restricted site of the defect also enables direct comparison with intact enthesis tissue in the same sample. Notably, both injury models are based on acute lacerations of healthy tendon and therefore do not recapitulate ruptures resulting from chronic degeneration.

To identify the source of scar forming cells, we used four inducible Cre lines to trace potential cell populations in the partial tear model, since the scar site can be simply defined. Although $Scx^{CreERT2}$ and $Sox9^{CreERT2}$ labeled differentiated tendon and cartilage/fibrocartilage cells, respectively, the scar cells in the injury site were not derived from these sources. This is consistent with recent studies showing that intrinsic cells of the articular

Author Manuscript Author Manuscript Author Manuscript Author Manuscript

cartilage (labeled with $Acan^{CreERT2}$) and mineralizing enthesis (labeled with $Gli1^{CreERT2}$) do not participate in enthesis healing.[22, 27] Although surrounding cells mount a limited proliferative response at day 7 after needle puncture enthesis injury, we observed limited proliferation at all timepoints assessed. This may indicate a fairly narrow window of proliferative activity. In our previous study of Achilles tendon transection injury, we observed that adult Scx^{lin} tendon cells are minimally proliferative at day 3 post-injury.[39] Similarly, other models challenging adult tenocytes *in vivo* showed that mature cells are largely quiescent after overuse or overloading with almost no proliferation.[43, 44] However, given the differences between supraspinatus and Achilles tendon healing, it may be that the temporal dynamics of proliferation are also different. Since the earliest timepoint investigated was at day 7, there may also be transient recruitment or turnover of Scx^{lin} or $Sox9^{lin}$ cells. To resolve these questions, timepoints prior to day 7 will be determined in future studies.

Surprisingly, lineage tracing using $\alpha SMA^{CreERT2}$ also failed to identify the source of scar-forming cells. αSMA is a general marker for myofibroblasts, a contractile cell type that is commonly activated during wound healing.[45] For tendon, αSMA is also expressed by epitenon cells surrounding the tendon proper (adult tenocytes do not normally express αSMA).[22, 39, 46] Using lineage tracing with $\alpha SMA^{CreERT2}$, it was shown that αSMA^{lin} cells are activated after patellar tendon injury and migrate into the defect.[42] In the Achilles tendon, αSMA+ cells (detected by immunostaining) are also rapidly recruited into the injury site after tendon transection, however it is unknown whether these cells are derived from the epitenon or another source.[39] A previous study tracing the fate of αSMA^{lin} cells in the rotator cuff showed expansion of these cells after partial supraspinatus tear, however these cells originate from the bursa covering the tendon and it is unclear whether these cells were detected in the local enthesis defect.[22, 46] Consistent with their findings, we also observed strong activation of αSMA^{lin} cells in the bursa and muscle, but little to no labeling was detected in tendon, epitenon, or enthesis. Since tamoxifen was given prior to injury, it is unknown whether scar forming cells may turn on αSMA after injury. However, immunostaining for αSMA did not show noticeable staining of scar cells after partial injury; the epitenon (which was clearly detectable by laminin and Sca1 immunostaining) also was not labeled by $\alpha SMA^{CreERT2}$. Taken together, these results indicate that healing of intra-articular (supraspinatus) vs extra-articular (Achilles, patellar) tendons may follow distinctive mechanisms. The unique loading environment of the supraspinatus may also play a role in regulating these disparate healing responses after injury.

To identify potential tissue resident stem cells in the enthesis or tendon, we then used $Axin2^{CreERT2}$ to label Wnt-responsive cells and found a subpopulation of labeled cells within the tendon body and almost no labeling of enthesis cells. Labeled tendon cells were observed throughout the tendon, suggesting that tendon stem/progenitor cells may reside within the tendon proper[28] and not within the epitenon[43] as has been suggested. However, co-labeling with epitenon marker laminin was not carried out and comprehensive characterization of $Axin2^{lin}$ tendon cells was also not determined in this study; the function of this subpopulation of tendon cells thus remains unknown. Although partial tear injury failed to elicit much response by $Axin2^{lin}$ cells, the full detachment/repair injury resulted in a large scar that was highly composed of $Axin2^{lin}$ cells. This difference in scar cells between

Author Manuscript Author Manuscript Author Manuscript Author Manuscript

injury models may suggest that the scar in the repair model is formed by cells recruited from the bone marrow. Or that the full detachment injury was severe enough to activate the *Axin2*^{lin} subpopulation from the tendon. Identifying the specific contribution of bone marrow cells will require a Cre line specific to bone marrow derived cells. Interestingly, labeling with *Sox9*^{CreERT2} showed that *Sox9*^{lin} cells and *Axin2*^{lin} cells occupied almost completely non-overlapping regions in the repair injury model. Although *Sox9* has also been used to identify stem cells of the nerve and hair follicles[47, 48], the distinctive labeling of nearly all enthesis fibrocartilage and tendon insertion cells indicates that in the context of the supraspinatus tendon, *Sox9* is a marker of differentiated cells rather than resident stem cells. Although we allowed one week of rest between tamoxifen injections and injury, this may not be sufficient to fully clear tamoxifen from the system as some reports indicated tamoxifen may persist even after two weeks for some inducible Cre lines.[49] Therefore, *Axin2*^{lin} cells detected in the repair may represent new cells that initiate *Axin2* expression, and are not necessarily derived from *Axin2*^{lin} cells, which is another exciting possibility.

Clinically, rotator cuff tendon injuries often lead to permanent damage to the adjacent muscle and bone. To detect bone loss, we measured overall bone mineral density of the humeral head using DEXA. While previous studies using microCT showed a detectable decrease in bone mineral density as an effect of unloading,[17, 50] our DEXA measurements did not detect such changes. This may be due to the lower resolution and sensitivity of DEXA compared to microCT. Partial tear injury also does not result in full unloading of the tendon; thus there may be minimal loss to bone. Other limitations include the absence of assays to assess fatty infiltration to muscle and muscle function. It is well established that these effects on muscle are clinically challenging and often irreversible. In mice, massive injuries of multiple rotator cuff tendons are usually used to induce detectable changes in muscle.[24] Future studies will therefore determine whether muscle impairment is observed with partial tear or full detachment/repair injuries. Similarly, while gait was carried out to determine overall limb function, direct mechanical testing would better assess intrinsic material properties of the healed tissue. Despite relatively normal gait in the partial tendon tear model, there may be persistent differences in mechanical properties of the tendon or tendon bone attachment. In addition, the results from quantitative cell counting for *Scx*^{lin} and *Sox9*^{lin} cells were not consistent with our qualitative assessment of histological sections, which consistently showed that the local scar defect contained very few labeled cells. This may be due to low sample size (n=4) as well as the large area of intact enthesis included in the region of interest. This could be overcome in future studies by defining separate regions of interest in the injured shoulder, and comparing the local defect site to the adjacent enthesis as well as to the contralateral control enthesis. Finally, analysis of the full detachment and repair model was limited to lineage tracing of two Cre lines at a single timepoint, with no analysis of cell proliferation dynamics. The massive scar formation observed with repair suggests that cell proliferation is likely to be far more intense compared to the partial defect model. Given the interesting differences between the injury models, ongoing studies will fully determine the temporal dynamics of proliferation and lineage tracing of *Scx*^{CreERT2} and *αSMA*^{CreERT2} lines to determine cell recruitment and potential turnover of these populations.

Author Manuscript Author Manuscript Author Manuscript Author Manuscript

Supplementary Material

Refer to Web version on PubMed Central for supplementary material.

ACKNOWLEDGMENTS

We thank Dr. Ronen Schweizer for providing the $Scx^{CreERT2}$ line and Dr Ivo Kalajzic for the $\alpha SMA^{CreERT2}$ line. We also acknowledge Christopher M. Smith for illustrations.

FUNDING

This study was supported by funding from the NIH/NIAMS (R01AR069537) to AHH and a fellowship from the Hans Neuenschwander Fond, Inselspital Bern to HM.

REFERENCES

1. Oh LS, Wolf BR, Hall MP, Levy BA, Marx RG. Indications for rotator cuff repair: a systematic review. Clin Orthop Relat Res. 2007;455:52–63. [PubMed: 17179786]
2. Soslowsky LJ, Thomopoulos S, Tun S, et al. Neer Award 1999. Overuse activity injures the supraspinatus tendon in an animal model: a histologic and biomechanical study. J Shoulder Elbow Surg. 2000;9:79–84. [PubMed: 10810684]
3. Economopoulos KJ, Brockmeier SF. Rotator cuff tears in overhead athletes. Clin Sports Med. 2012;31:675–692. [PubMed: 23040553]
4. Song N, Armstrong AD, Li F, Ouyang H, Niyibizi C. Multipotent mesenchymal stem cells from human subacromial bursa: potential for cell based tendon tissue engineering. Tissue Eng Part A. 2014;20:239–249. [PubMed: 23865619]
5. Kim SJ, Song DH, Park JW, Park S, Kim SJ. Effect of Bone Marrow Aspirate Concentrate-Platelet-Rich Plasma on Tendon-Derived Stem Cells and Rotator Cuff Tendon Tear. Cell Transplant. 2017;26:867–878. [PubMed: 28105983]
6. Yin Z, Chen X, Zhu T, et al. The effect of decellularized matrices on human tendon stem/progenitor cell differentiation and tendon repair. Acta Biomater. 2013;9:9317–9329. [PubMed: 23896565]
7. Patel S, Gualtieri AP, Lu HH, Levine WN. Advances in biologic augmentation for rotator cuff repair. Ann N Y Acad Sci. 2016;1383:97–114. [PubMed: 27750374]
8. Gerber C, Wirth SH, Farshad M. Treatment options for massive rotator cuff tears. J Shoulder Elbow Surg. 2011;20:S20–29. [PubMed: 21281919]
9. Galatz LM, Ball CM, Teefey SA, Middleton WD, Yamaguchi K. The outcome and repair integrity of completely arthroscopically repaired large and massive rotator cuff tears. J Bone Joint Surg Am. 2004;86-A:219–224. [PubMed: 14960664]
10. Harryman DT, 2nd, Mack LA, Wang KY, Jackins SE, Richardson ML, Matsen FA, 3rd. Repairs of the rotator cuff. Correlation of functional results with integrity of the cuff. J Bone Joint Surg Am. 1991;73:982–989. [PubMed: 1874784]
11. Mather RC, 3rd, Koenig L, Acevedo D, et al. The societal and economic value of rotator cuff repair. J Bone Joint Surg Am. 2013;95:1993–2000. [PubMed: 24257656]
12. Zelzer E, Blitz E, Killian ML, Thomopoulos S. Tendon-to-bone attachment: from development to maturity. Birth Defects Res C Embryo Today. 2014;102:101–112. [PubMed: 24677726]
13. Thomopoulos S, Genin GM, Galatz LM. The development and morphogenesis of the tendon-to-bone insertion - what development can teach us about healing. J Musculoskelet Neuronal Interact. 2010;10:35–45. [PubMed: 20190378]
14. Thangarajah T, Pendegrass CJ, Shahbazi S, Lambert S, Alexander S, Blunn GW. Augmentation of Rotator Cuff Repair With Soft Tissue Scaffolds. Orthop J Sports Med. 2015;3:2325967115587495. [PubMed: 26665095]
15. Derwin KA, Baker AR, Iannotti JP, McCarron JA. Preclinical models for translating regenerative medicine therapies for rotator cuff repair. Tissue Eng Part B Rev. 2010;16:21–30. [PubMed: 19663651]

Author Manuscript Author Manuscript Author Manuscript Author Manuscript

16. Galatz LM, Rothermich SY, Zaegel M, Silva MJ, Havlioglu N, Thomopoulos S. Delayed repair of tendon to bone injuries leads to decreased biomechanical properties and bone loss. J Orthop Res. 2005;23:1441–1447. [PubMed: 16055296]
17. Killian ML, Cavinatto LM, Ward SR, Havlioglu N, Thomopoulos S, Galatz LM. Chronic Degeneration Leads to Poor Healing of Repaired Massive Rotator Cuff Tears in Rats. Am J Sports Med. 2015;43:2401–2410. [PubMed: 26297522]
18. Cohen DB, Kawamura S, Ehteshami JR, Rodeo SA. Indomethacin and celecoxib impair rotator cuff tendon-to-bone healing. Am J Sports Med. 2006;34:362–369. [PubMed: 16210573]
19. Reuther KE, Tucker JJ, Thomas SJ, et al. Effect of scapular dyskinesis on supraspinatus repair healing in a rat model. J Shoulder Elbow Surg. 2015;24:1235–1242. [PubMed: 25745826]
20. Beason DP, Tucker JJ, Lee CS, Edelstein L, Abboud JA, Soslowsky LJ. Rat rotator cuff tendon-to-bone healing properties are adversely affected by hypercholesterolemia. J Shoulder Elbow Surg. 2014;23:867–872. [PubMed: 24295837]
21. Bell R, Taub P, Cagle P, Flatow EL, Andarawis-Puri N. Development of a mouse model of supraspinatus tendon insertion site healing. J Orthop Res. 2015;33:25–32. [PubMed: 25231092]
22. Yoshida R, Alaee F, Dyrna F, et al. Murine supraspinatus tendon injury model to identify the cellular origins of rotator cuff healing. Connect Tissue Res. 2016;57:507–515. [PubMed: 27184388]
23. Lebaschi A, Nakagawa Y, Wada S, Cong GT, Rodeo SA. Tissue-specific endothelial cells: a promising approach for augmentation of soft tissue repair in orthopedics. Ann N Y Acad Sci. 2017;1410:44–56. [PubMed: 29265420]
24. Kuenzler MB, Nuss K, Karol A, et al. Neer Award 2016: reduced muscle degeneration and decreased fatty infiltration after rotator cuff tear in a poly(ADP-ribose) polymerase 1 (PARP-1) knock-out mouse model. J Shoulder Elbow Surg. 2017;26:733–744. [PubMed: 28131694]
25. Dyment NA, Breidenbach AP, Schwartz AG, et al. Gdf5 progenitors give rise to fibrocartilage cells that mineralize via hedgehog signaling to form the zonal enthesis. Dev Biol. 2015;405:96–107. [PubMed: 26141957]
26. Schwartz AG, Long F, Thomopoulos S. Enthesis fibrocartilage cells originate from a population of Hedgehog-responsive cells modulated by the loading environment. Development. 2015;142:196–206. [PubMed: 25516975]
27. Schwartz AG, Galatz LM, Thomopoulos S. Enthesis regeneration: a role for Gli1+ progenitor cells. Development. 2017;144:1159–1164. [PubMed: 28219952]
28. Bi Y, Ehirchiou D, Kilts TM, et al. Identification of tendon stem/progenitor cells and the role of the extracellular matrix in their niche. Nat Med. 2007;13:1219–1227. [PubMed: 17828274]
29. Tsai CC, Huang TF, Ma HL, Chiang ER, Hung SC. Isolation of mesenchymal stem cells from shoulder rotator cuff: a potential source for muscle and tendon repair. Cell Transplant. 2013;22:413–422. [PubMed: 23006509]
30. Nagura I, Kokubu T, Mifune Y, et al. Characterization of progenitor cells derived from torn human rotator cuff tendons by gene expression patterns of chondrogenesis, osteogenesis, and adipogenesis. J Orthop Surg Res. 2016;11:40. [PubMed: 27036202]
31. Utsunomiya H, Uchida S, Sekiya I, Sakai A, Moridera K, Nakamura T. Isolation and characterization of human mesenchymal stem cells derived from shoulder tissues involved in rotator cuff tears. Am J Sports Med. 2013;41:657–668. [PubMed: 23371475]
32. van Amerongen R, Bowman AN, Nusse R. Developmental stage and time dictate the fate of Wnt/beta-catenin-responsive stem cells in the mammary gland. Cell Stem Cell. 2012;11:387–400. [PubMed: 22863533]
33. Barker N, van Es JH, Kuipers J, et al. Identification of stem cells in small intestine and colon by marker gene Lgr5. Nature. 2007;449:1003–1007. [PubMed: 17934449]
34. Jaks V, Barker N, Kasper M, et al. Lgr5 marks cycling, yet long-lived, hair follicle stem cells. Nat Genet. 2008;40:1291–1299. [PubMed: 18849992]
35. Lehoczky JA, Tabin CJ. Lgr6 marks nail stem cells and is required for digit tip regeneration. Proc Natl Acad Sci U S A. 2015;112:13249–13254. [PubMed: 26460010]

Author Manuscript Author Manuscript Author Manuscript Author Manuscript

36. Kopp JL, Dubois CL, Schaffer AE, et al. Sox9+ ductal cells are multipotent progenitors throughout development but do not produce new endocrine cells in the normal or injured adult pancreas. Development. 2011;138:653–665. [PubMed: 21266405]

37. Grcevic D, Pejda S, Matthews BG, et al. In vivo fate mapping identifies mesenchymal progenitor cells. Stem Cells. 2012;30:187–196. [PubMed: 22083974]

38. Madisen L, Zwingman TA, Sunkin SM, et al. A robust and high-throughput Cre reporting and characterization system for the whole mouse brain. Nat Neurosci. 2010;13:133–140. [PubMed: 20023653]

39. Howell K, Chien C, Bell R, et al. Novel Model of Tendon Regeneration Reveals Distinct Cell Mechanisms Underlying Regenerative and Fibrotic Tendon Healing. Sci Rep. 2017;7:45238. [PubMed: 28332620]

40. R Core Team (2018). R: A language and environment for statistical computing. In: Vienna ARFfSC, ed 2018.

41. Bates D, Mächler M, Bolker B, and Walker S Fitting Linear Mixed-Effects Models Using lme4. Journal of Statistical Software. 2015;67:1–48.

42. Dyment NA, Liu CF, Kazemi N, et al. The paratenon contributes to scleraxis-expressing cells during patellar tendon healing. PLoS One. 2013;8:e59944. [PubMed: 23555841]

43. Mendias CL, Gumucio JP, Bakhurin KI, Lynch EB, Brooks SV. Physiological loading of tendons induces scleraxis expression in epitenon fibroblasts. J Orthop Res. 2012;30:606–612. [PubMed: 21913219]

44. Andarawis-Puri N, Flatow EL. Tendon fatigue in response to mechanical loading. J Musculoskelet Neuronal Interact. 2011;11:106–114. [PubMed: 21625047]

45. Darby I, Skalli O, Gabbiani G. Alpha-smooth muscle actin is transiently expressed by myofibroblasts during experimental wound healing. Lab Invest. 1990;63:21–29. [PubMed: 2197503]

46. Dyment NA, Hagiwara Y, Matthews BG, Li Y, Kalajzic I, Rowe DW. Lineage tracing of resident tendon progenitor cells during growth and natural healing. PLoS One. 2014;9:e96113. [PubMed: 24759953]

47. Furuyama K, Kawaguchi Y, Akiyama H, et al. Continuous cell supply from a Sox9-expressing progenitor zone in adult liver, exocrine pancreas and intestine. Nat Genet. 2011;43:34–41. [PubMed: 21113154]

48. Snippert HJ, Clevers H. Tracking adult stem cells. EMBO Rep. 2011;12:113–122. [PubMed: 21252944]

49. Reinert RB, Kantz J, Misfeldt AA, et al. Tamoxifen-Induced Cre-loxP Recombination Is Prolonged in Pancreatic Islets of Adult Mice. PLoS One. 2012;7:e33529. [PubMed: 22470452]

50. Killian ML, Cavinatto L, Shah SA, et al. The effects of chronic unloading and gap formation on tendon-to-bone healing in a rat model of massive rotator cuff tears. J Orthop Res. 2014;32:439–447. [PubMed: 24243733]

Author Manuscript Author Manuscript Author Manuscript Author Manuscript

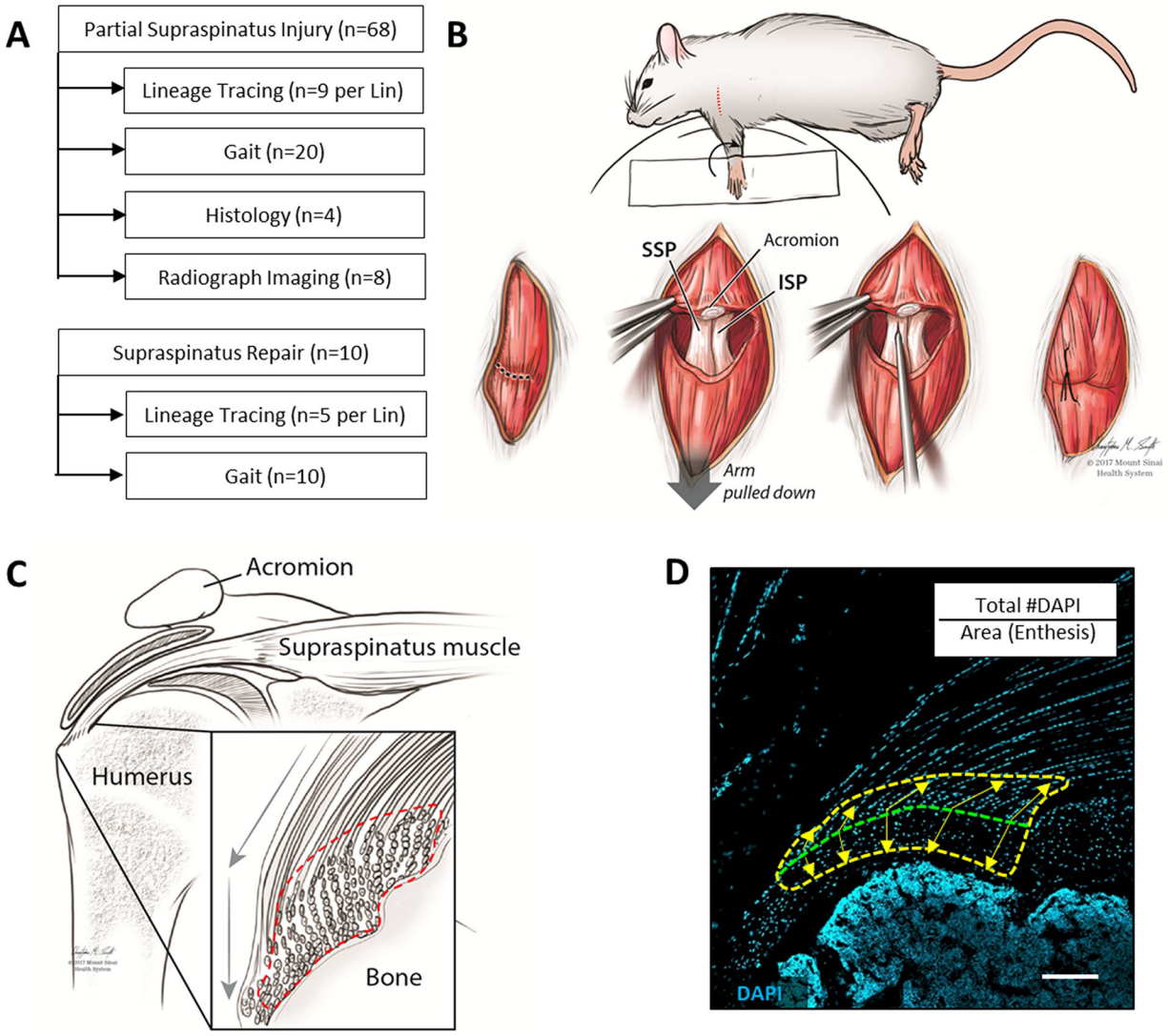

Figure 1: Experimental design and methods overview.

(**A**) Experimental design and sample size for supraspinatus injury models. (**B**) Schematic demonstrating partial supraspinatus tendon tear surgery. (**C**) Schematic and (**D**) DAPI-stained histological section of the supraspinatus tendon defining the enthesis region of interest used for cell quantification (dotted lines). Transition between mineralized and unmineralized fibrocartilage is indicated by the green dotted line and equidistant points extending toward bone and tendon used to define the outer boundaries of the region of interest (yellow arrows). Scalebar: 100μm.

Author Manuscript Author Manuscript Author Manuscript Author Manuscript

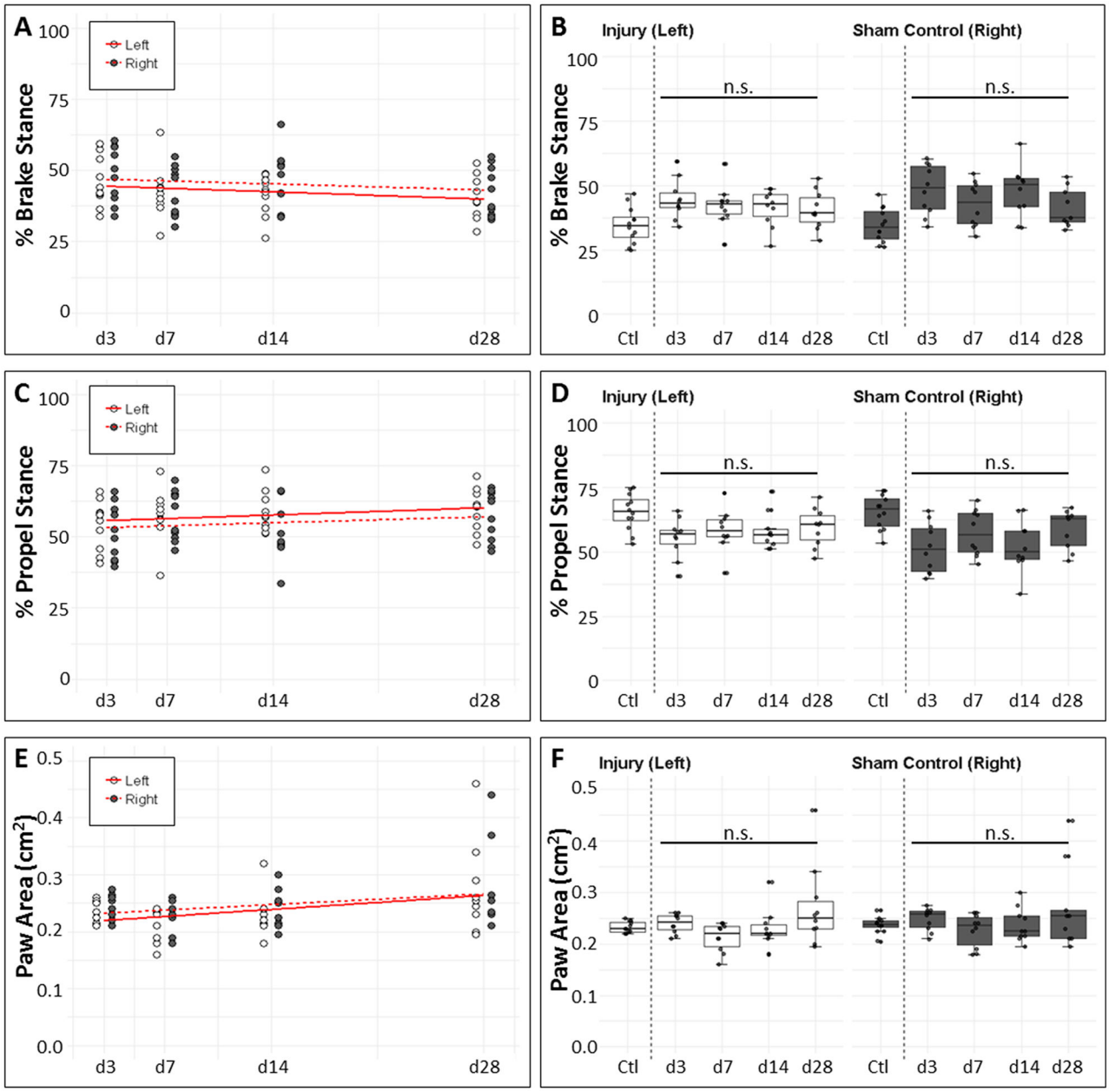

Figure 2: Minor impairment of functional gait after partial supraspinatus tear.

(**A**, **B**) %BrakeStance and (**C**, **D**) %PropelStance were not significantly different between (**A**, **C**) injury and sham control limbs or (**B**, **D**) limbs from non-injured and injured mice. (**E**) PawArea significantly increased over time post-surgery (p=0.013). (**F**) PawArea between uninjured (d0) and injured animals were not significantly different at any timepoint (p>0.05). n.s. indicates not significant (p>0.05).

Author Manuscript Author Manuscript Author Manuscript Author Manuscript

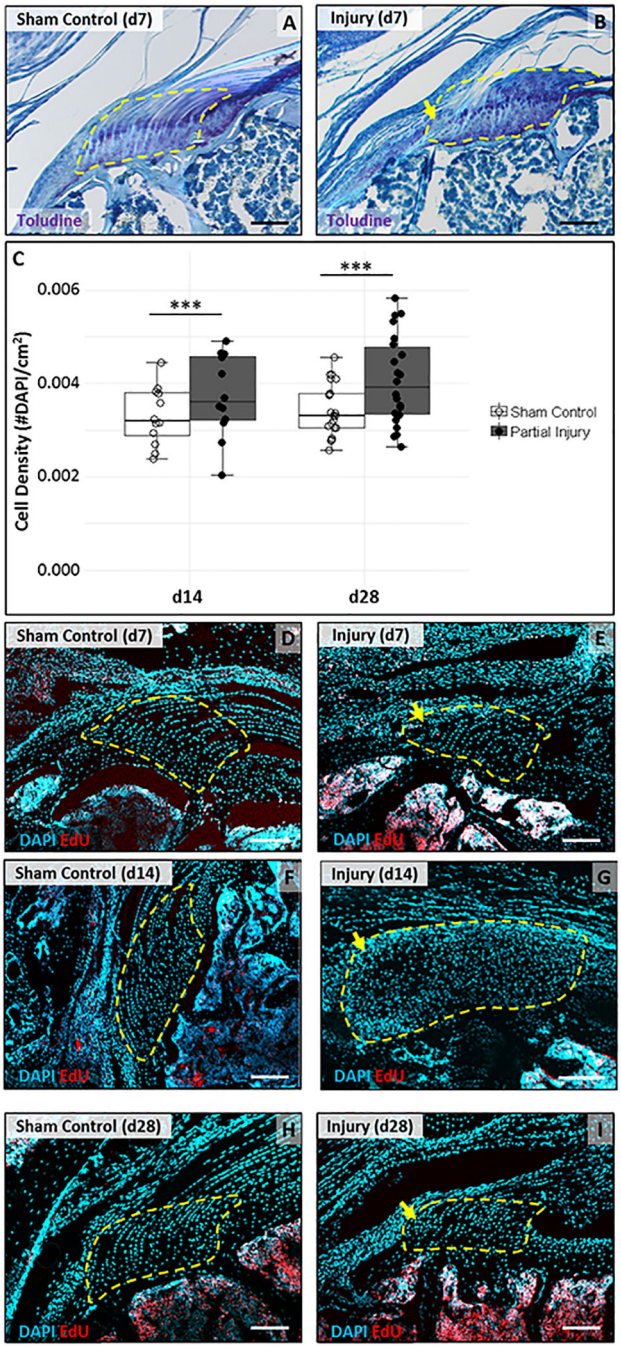

Figure 3: Loss of enthesis architecture and hypercellular scar formation after partial supraspinatus tear.

(**A**, **B**) Toluidine blue staining of supraspinatus tendon sections show loss of enthesis structure in the localized defect by d7. (**C**) Quantification of DAPI stained sections show increase in cell density at d14 and d28 (n=12–22). *** indicates significant difference ($p<0.001$). DAPI and EdU detection of supraspinatus tendon sections show very limited cell proliferation in the scar at (**D**, **E**) d7 and no proliferation at (**F**, **G**) d14 or (**H**, **I**) d28.

Author Manuscript Author Manuscript Author Manuscript Author Manuscript

Localized enthesis scar indicated by yellow arrows. Region of interest highlighted by yellow dashed outlines. Scalebars: 100um.

Author Manuscript Author Manuscript Author Manuscript Author Manuscript

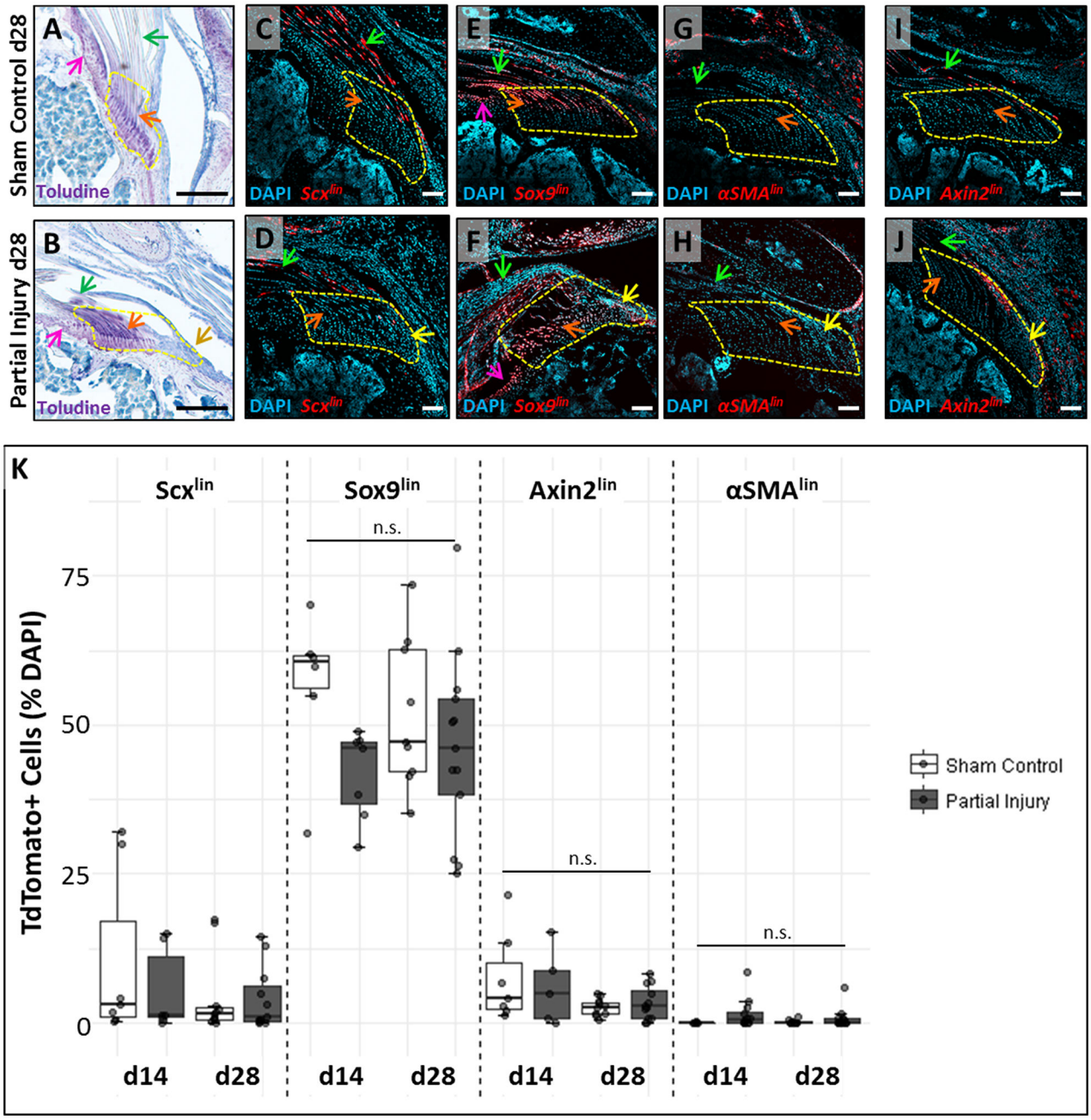

Figure 4: Lineage tracing does not identify the source of enthesis scar cells.

(**A**, **B**) Toluidine blue staining of supraspinatus tendon sections show sustained loss of enthesis structure in the localized defect at d28. Lineage tracing using (**C**, **D**) *Scx*^{CreERT2}, (**E**, **F**) *Sox9*^{CreERT2}, (**G**, **H**) *αSMA*^{CreERT2}, and (**I**, **J**) *Axin2*^{CreERT2} did not show observable contribution of TdTomato+ cells to the scar defect. (**K**) Quantification of %TdTomato cells in the region of interest. n.s. indicates not significantly different ($p>0.05$). Arrows indicate: tendon (green), un-mineralized enthesis fibrocartilage (orange), scar (yellow), and articular cartilage (pink). White scalebars: 100um. Black scalebars: 200um.

Author Manuscript Author Manuscript Author Manuscript Author Manuscript

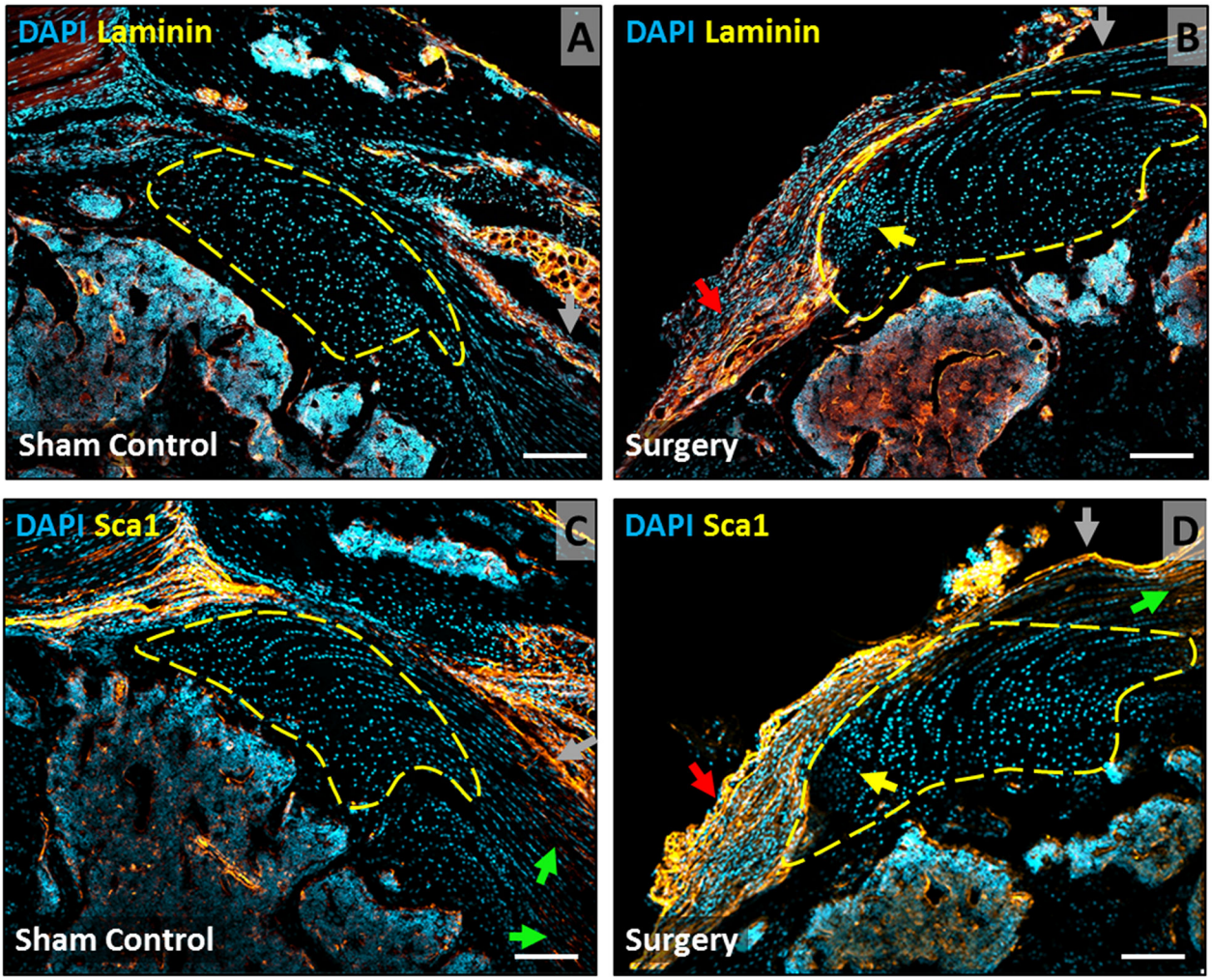

Figure 5: Laminin and Sca1 immunostaining shows expansion of bursa at d28 after injury.
Immunostaining for (**A**, **B**) laminin and (**C**, **D**) Sca1 in supraspinatus tendon sections at d28 highlight epitenon, bursa, and bone marrow cells, with no staining of enthesis fibrocartilage or scar cells. Arrows indicate: enthesis scar (yellow), bursa (red), tendon (green), epitenon (gray). Scalebars: 100um.

Author Manuscript Author Manuscript Author Manuscript Author Manuscript

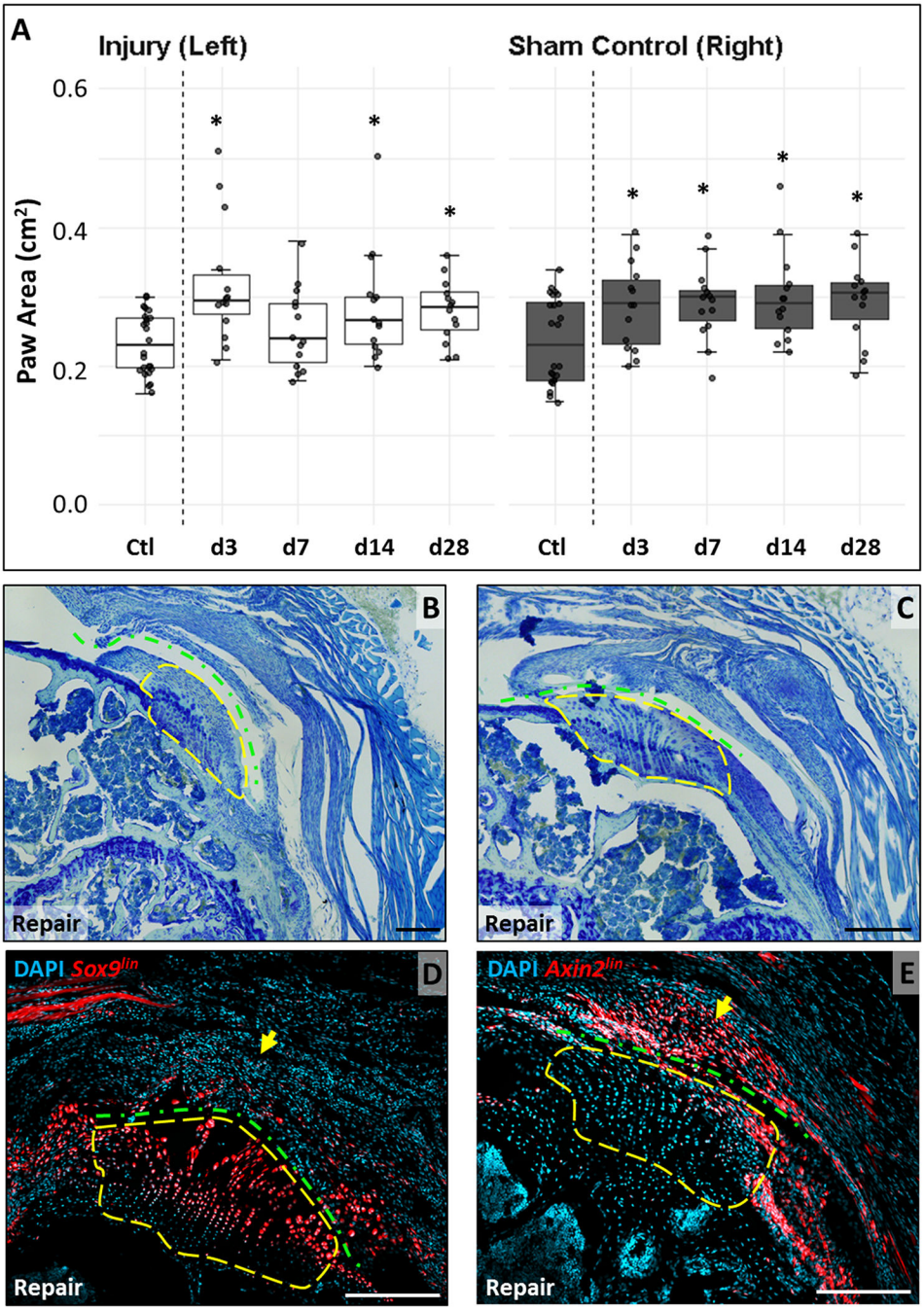

Figure 6: Full tendon detachment and repair results in functional changes and recruitment of *Axin*^{lin} scar cells.

(A) Paw area is generally significantly increased in both limbs of injured animals compared to limbs of non-injured animals. (**B**, **C**) Toluidine blue staining of supraspinatus tendon sections show disruption of enthesis organization and characteristic orientation with massive scar formation. Lineage tracing using (**D**) *Sox9*^{CreERT2} shows *TdTomato*+ cells in enthesis fibrocartilage with no labeling in the scar. (**E**) *Axin2*^{CreERT2} tracing shows little labeling of enthesis fibrocartilage but considerable presence of *TdTomato*+ cells in the scar. Yellow

dashed outlines enclose similar regions. Green dashed line indicates detachment site. Black scalebars: 200μm. White scalebars: 100μm.

Author Manuscript Author Manuscript Author Manuscript Author Manuscript